2
Fabrication and Characterization Techniques

For any experiment to be a success, one of the most important roles is played by the choice of fabrication, characterization, analytical tools and methods. Several factors, such as time, temperature, environment, and performance, must be considered when selecting techniques. To provide detailed and crucial insights on device performance, the fabrication, characterization, and analytical techniques are critical criteria. Additionally, after characterizing the materials, films, and devices, extracting required parameters from the raw data is vital to determine the mechanism. This chapter provides an overview of the various fabrication, characterization, and data extraction techniques for RRAM devices employed in this thesis.

2.1 Fabrication of flexible RRAM device

For the fabrication of flexible RRAM devices, the ambient conditions must be stable as these devices are highly sensitive to environmental fluctuations such as humidity, temperature, light, and moisture. In this research, ITO coated PET/PEN substrates were used to fabricate flexible devices. All materials were procured from Sigma-Aldrich, Inc. and used without further purification. The fabrication process of flexible RRAMs commenced with the thorough cleaning of ITO coated substrates. The PET/PEN substrates were cleaned using an ultrasonic bath, sequentially immersed in 2-propanol, acetone, de-ionized (DI) water, and methanol for 15 minutes each in an ultrasonicator system. The digital image of ultrasonic cleaner from Rivotek is shown in Figure 2.1.



Figure 2.1 Digital image of ultrasonic cleaner

Finally, a high-pressure N_2 blow was utilized to remove any remaining moisture and dust from the substrates. Throughout our research, the flexible RRAM devices were fabricated using the very simple common BE structure method. This means that the BE was shared with all circular TEs on a single substrate. Figure 2.2(a) show the schematic structure of the fabricated device.

In the fabrication of flexible RRAM devices using ITO-coated PET/PEN substrates, the ITO layer functioned as the BE. TEs (Ag) were deposited through a shadow mask in a thermal evaporation system. The switching layer was constructed using one of three approaches: a single polymer or solution-processed 2D materials layer, a composite layer of 2D materials and polymer, or a hybrid bilayer. In the hybrid bilayer approach, one layer consisted of either a single or composite 2D material with polymer, while the second layer was composed of metal oxide materials. Figure 2.2(b), shows the digital image of the fabricated flexible RRAM device. Throughout the fabrication process and subsequent stages, various characterization techniques

were employed for these devices. Ultraviolet-visible diffuse reflectance spectroscopy (UV-Vis DRS) was used to analyse the energy band gap of the switching layer materials, atomic force microscopy (AFM) using the SPM XE-70 instrument from Park Systems was utilized to capture the surface morphologies of the crystals. The effect of temperature on properties of switching layer materials and their thermal stability were analyzed by thermogravimetric analysis (TGA) with Perkin Elmor STA 6000 and through differential scanning calorimetry (DSC) by Perkin Elmor DSC 4200 system. Electrical measurements were conducted using the Keithley 4200 SCS parameter analyzer in combination with a probe station. The following section provides a detailed overview of the different fabrication tools and analytical methods employed, as discussed in the preceding section.

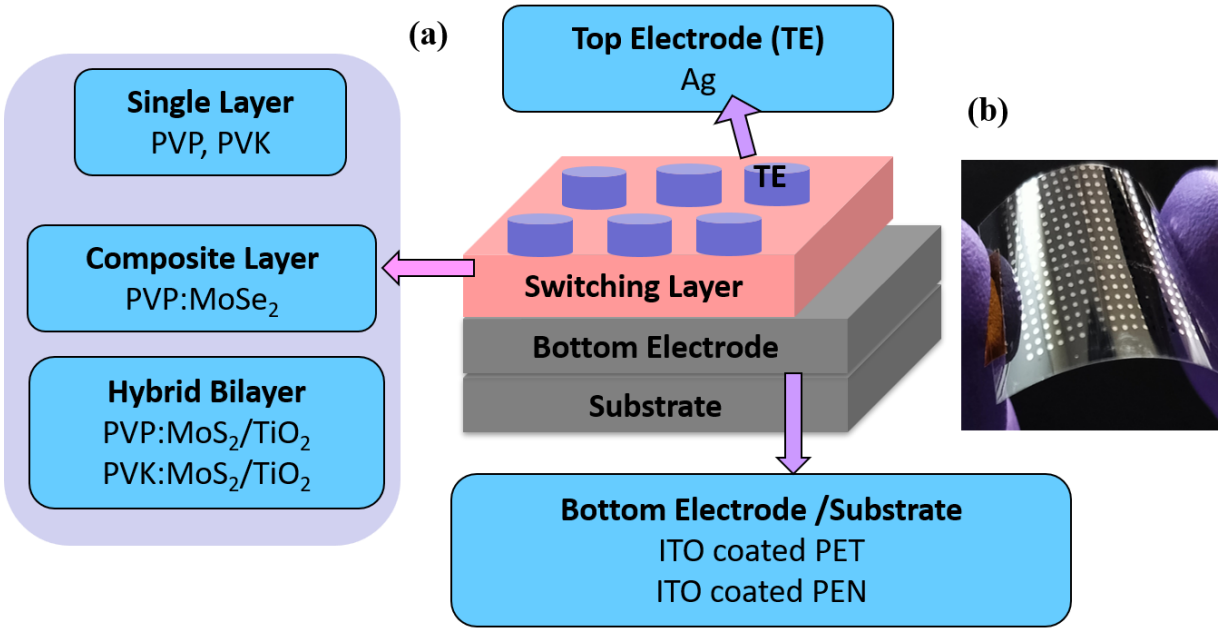


Figure 2.2 (a) Schematic structure and **(b)** digital image of the fabricated device.

2.2 Spin Coating

Spin coating is a prevalent, cost-effective, low-temperature technique which is widely utilized for solution-processable thin film deposition, particularly suitable for flexible substrate devices. In this process, the material to be coated is mixed with an appropriate solvent, stirred or ultrasonicated, and then spin-coated onto the ITO-coated BE at varying rotation speeds to achieve the desired thickness. Centrifugal forces spread the solution across the surface, forming a thin and uniform film. After spin coating, the solution is either annealed or allowed to evaporate completely. Film thickness is influenced by factors such as solution viscosity, solvent evaporation rate, material density in the solution, time duration of rotation, rotation acceleration, and the position of sample. The main advantages of spin coating include its simple setup, ease of use, low maintenance, affordability, and rapid production of uniform thin films. However, it is a batch process with low throughput, and the short drying time of the film can pose challenges in producing self-assembled or crystalline coatings. Additionally, only a small amount of the material is used for deposition, with the remainder wasted. In this study, the spin coating method was employed for the deposition of 2D materials and its composites with polymers. The spin coating system used was the HO-THOSC from HOLMARC. The deposition speed was varied from 1000 to 4000 rpm with rotation times between 30 to 45 seconds. After deposition, the samples were annealed at suitable temperature for removing the residual impurities. Figure 2.3(a-d) illustrate the deposition process using a schematic and Figure 2.3(e), shows the digital image of the spin coater system, respectively. A cleaned substrate is placed at the center of the spin coater, and the solution is spread using a syringe. The lid of the spin coater is then closed, and the desired

speed and duration are set. After the rotation is complete, the sample is dried on a hot plate at the specified temperature.

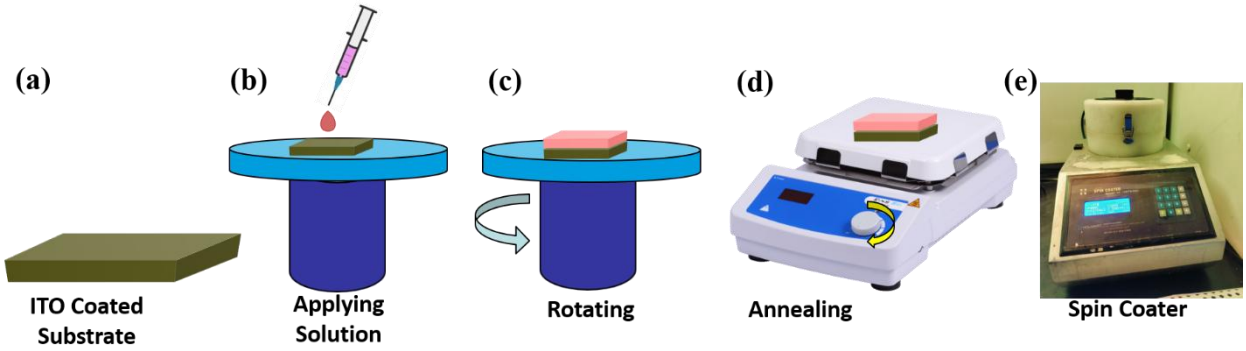


Figure 2.3 (a-d) Schematic illustration of thin film deposition using spin coating technique, and **(e)** Digital image of the HOLMARC spin coater.

2.3 Thermal Evaporation

Thermal evaporation is a widely used as a physical vapor deposition technique for fabricating metal electrodes. It relies on resistive heating to raise the temperature of a source material beyond its melting point, transforming it into vapor. The vaporized material then travels through a vacuum and condenses on a sample through required device shadow mask, forming a thin metallic contact.

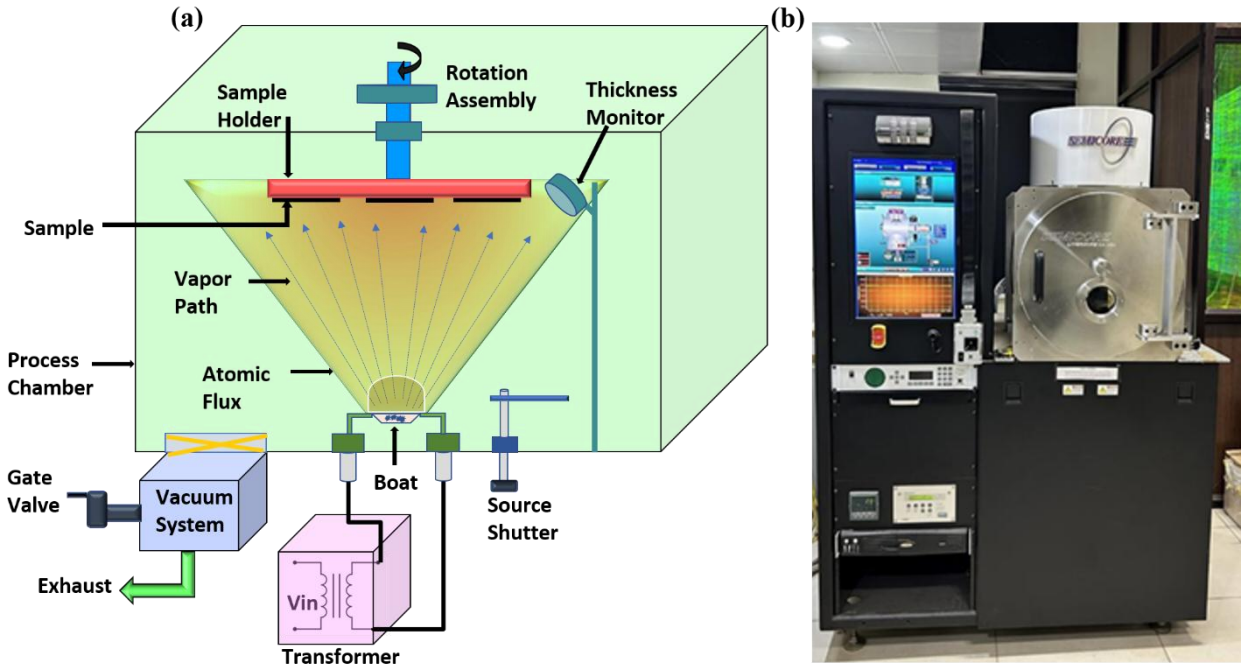


Figure 2. 4 (a) Schematic illustration and **(b)** Digital image of thermal evaporation system.

Typically, a tungsten boat serves as the heating container, which is heated using a high electric current. The process takes place in a high-vacuum environment, usually exceeding 10^{-6} Torr, achieved through vacuum pumping systems. These conditions maximize the mean free path of the evaporated particles, allowing them to travel to the sample without significant collisions with residual gas molecules, thereby improving the purity of the deposited metallic contacts. In the experimental setup, the tungsten boat connected to a power source is placed at the bottom of the chamber, while the sample with shadow mask attached are positioned above it, directly facing the boat. A schematic diagram of the thermal evaporation process is shown in Figure 2.4 (a) and a digital image of the thermal evaporation system is presented in Figure 2.4(b). This technique was employed in our study to deposit silver (Ag) as TEs. The system operated

under a vacuum pressure of less than 10^{-6} Torr. A stylus profilometer was used to measure the film thickness. In our RRAM devices, TEs (Ag) were deposited with a thickness of ~ 200 nm.

2.4 Atomic Layer Deposition

Atomic layer deposition (ALD) is a thin film deposition process that enables the deposition of atomically thin films of various materials, including oxides, nitrides, sulfides, metals, and fluorides, with precise stoichiometric control. Additionally, ALD allows for doping and the growth of films in nano-laminate and nano-structured forms. This technique is renowned for producing highly conformal films on high aspect-ratio structures, ensuring uniform and precise thickness control, adjustable stoichiometry, and films with minimal defects.

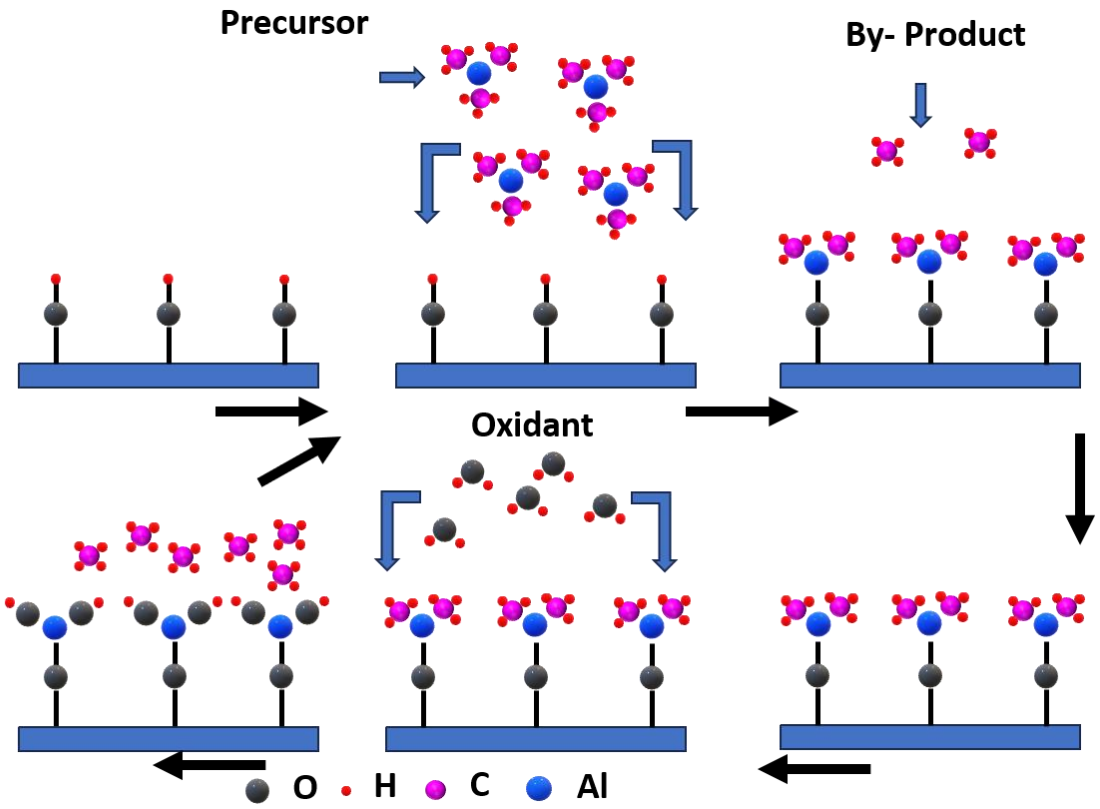


Figure 2.5 Schematic illustration of one complete cycle of ALD.

The deposition process involves self-limiting reactions of precursor molecules, which are transported into the reaction chamber by an inert carrier gas through alternating pulses designed for the specific precursor process. During the first half-cycle, the first precursor vapours are introduced into the chamber for a brief period, where they react with the substrate surface to form a monolayer. Adequate time is allowed for the precursor to react with the substrate surface, while by-products are simultaneously removed from the chamber using purge gases. The second half-cycle involves pulsing and purging the second precursor, which reacts with the first to form the monolayer of the desired material. This process is repeated multiple times in the vacuum chamber (less than 1 Torr) to achieve the desired thickness, as illustrated in Figure 2.5. This thesis research was conducted using the Savannah S200 ALD system from Cambridge Nanotech, as depicted in Figure 2.6(a). In this study, high-k dielectric TiO_2, using tetrakis(dimethylamido)titanium(IV) (TDT) and H_2O as precursors, were deposited on both rigid and flexible substrates at 150 °C. Figure 2.6(b) illustrates the machine schematic for TiO_2 deposition using TDT and H_2O precursors.

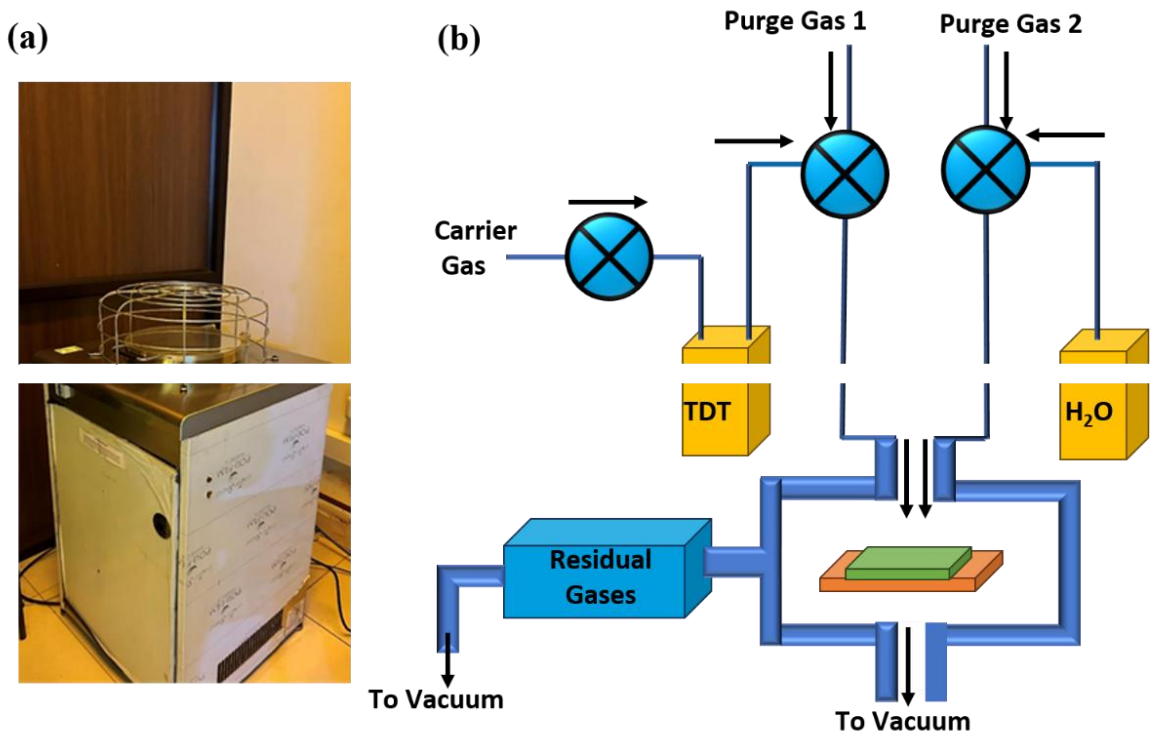


Figure 2.6 (a) Digital image of the Savannah S200 ALD system and **(b)** schematic process flow of ALD system.

2.5 Ultra-Violet and Visible Diffuse Reflectance Spectroscopy (UV-Vis DRS)

Ultraviolet-visible spectroscopy (UV-visible spectroscopy) is a widely utilized analytical technique for investigating the optical properties of liquid and solid materials. This method examines the interaction of light with matter over the spectral range of 200–800 nm.

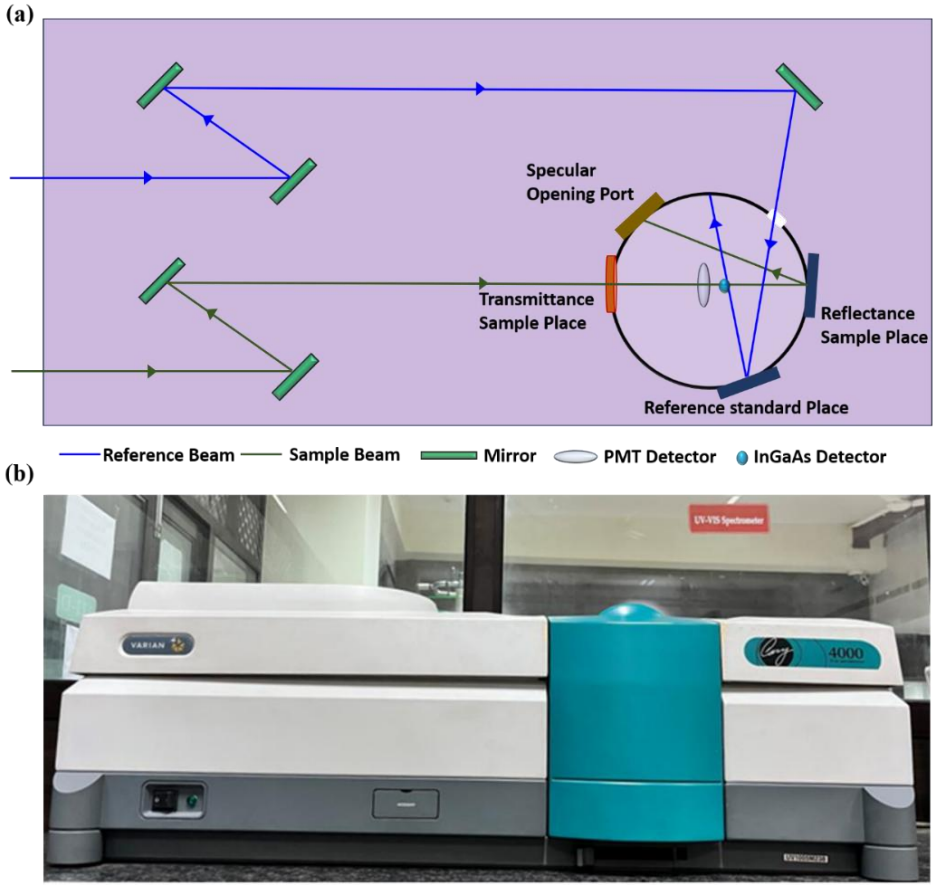
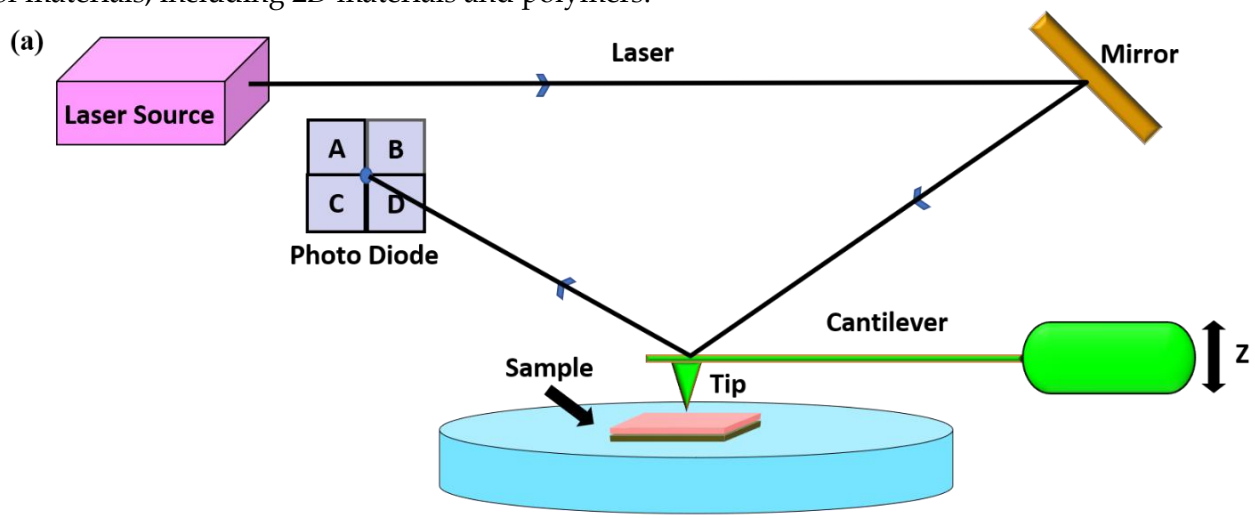


Figure 2.7 (a) Schematic and **(b)** digital image of the UV-Vis Spectrometer.

The high-energy ultraviolet and visible radiation in this range induces electronic transitions, where electrons move from lower to higher energy states. The principles of UV-visible spectroscopy are governed by the Beer-Lambert law, which establishes a linear relationship between the absorbance of a solution, the concentration of the absorbing species, and the optical path length. Consequently, for a given path length, the concentration of the absorber in a solution can be accurately determined using this technique. A UV-visible spectrometer typically consists of a light source capable of emitting radiation in both the ultraviolet and visible regions of the electromagnetic spectrum. The absorption of UV or visible light by the sample generates a characteristic spectrum that aids in the identification and classification of compounds. A key component of the spectrometer is the monochromator, which isolates specific wavelengths from the emitted light using a diffraction grating or prism while blocking other wavelengths. In this study, UV-visible spectroscopy was employed to analyze samples over a wavelength range of 200–800 nm. Figure 2.7 (a & b) show the schematic representation of the working principle and the digital image of UV-visible spectrometer (Perkin Elmer) utilized for the experimental work.

2.6 Atomic Force Microscopy (AFM)

The atomic force microscope (AFM) has emerged as one of the most advanced and widely utilized techniques for nanoscale surface characterization, offering high-resolution, three-dimensional imaging capabilities. AFM is highly versatile, allowing the analysis of a wide range of materials, including 2D materials and polymers.



(b)

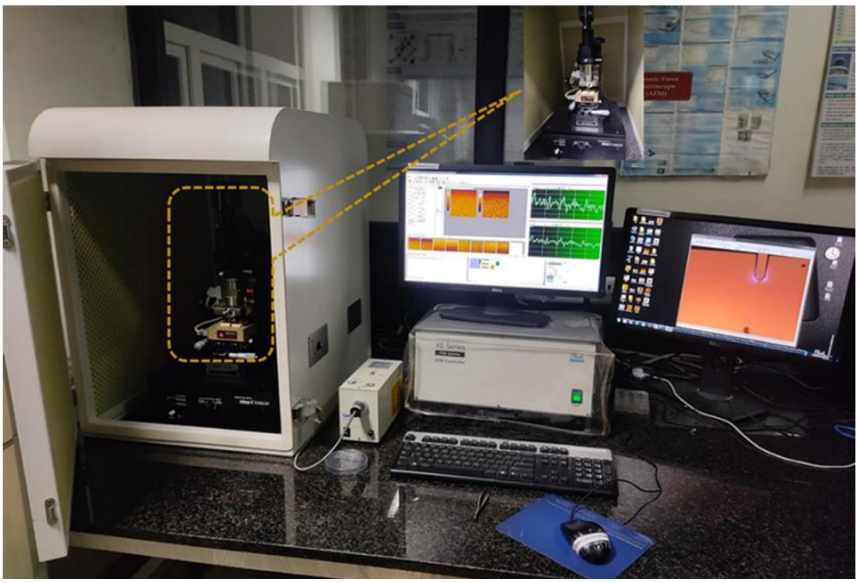


Figure 2.8 (a) Schematic and **(b)** digital image of the AFM.

The AFM scanning process utilizes a cantilever with a sharp tip, typically 10–20 nm in diameter, which traverses the sample surface in a precise raster pattern. As the tip approaches the sample, ionic repulsive forces induce upward deflection of the cantilever. These forces are quantified by measuring the extent of the cantilever's deflection, determined via the reflection of a laser beam onto a position-sensitive photodetector (PSPD). The separation between the tip and the sample surface, defined as the setpoint, is actively maintained at a constant value using a feedback control loop to ensure accurate imaging. The PSPD is highly sensitive, capable of detecting cantilever deflections as minute as 0.1 Å, enabling precise surface characterization. During the scan, the vertical motion of the cantilever tip corresponds to the surface topography, as the AFM maintains a constant interaction force between the tip and the sample. The resultant data enables the generation of a high-resolution surface profile. In this study, the Park Systems SPM XE-70 instrument was employed for surface morphologies in non-contact (tapping) mode. Figure 2.8(a) shows the operational principle of AFM scanning and imaging, while Figure 2.8(b) presents a digital image of the system used in the research. The topographic images were subjected to detailed analysis to derive comprehensive morphological parameters.

2.7 Raman Spectroscopy

Raman spectroscopy is an advanced analytical technique used to qualitatively and quantitatively study covalently bonded molecules by analyzing their vibrational modes. It relies on the Raman effect, which describes the wavelength shift of monochromatic light upon interaction with molecular vibrations, unique to each molecule. Raman spectroscopy effectively characterizes symmetric molecules, such as H_2, N_2, and O_2, by probing their vibrational transitions.

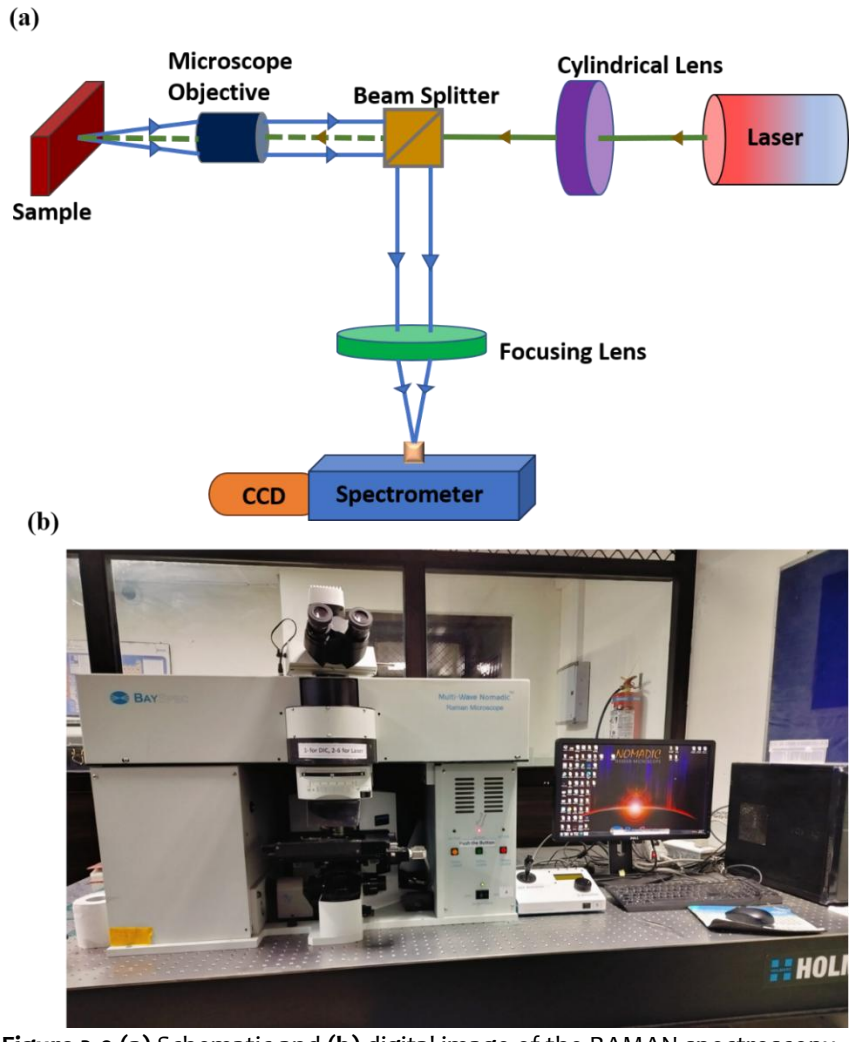


Figure 2.9 (a) Schematic and **(b)** digital image of the RAMAN spectroscopy.

When monochromatic light interacts with a sample, it scatters in various directions. The scattered light may retain the same frequency as the incident beam (Rayleigh scattering), exhibit a lower frequency (Stokes scattering), or a higher frequency (Anti-Stokes scattering) relative to the incident light. The frequencies of the Stokes and Anti-Stokes lines are determined by the vibrational modes of the molecule. A Raman spectrometer consists of key components such as a sample excitation laser, optical elements for directing light onto the sample and collecting scattered light, a wavelength-specific filter, and a charge-coupled device (CCD) detector. During operation, a Nd:YAG laser irradiates the sample, and the scattered light is collimated by a lens system before being analyzed by the spectrometer to produce the Raman spectrum. Due to the inherently weak nature of Raman scattering, separating the Raman signal from the dominant Rayleigh scattering is a critical challenge. To address this, tuneable or notch filters are employed to isolate the Stokes and Anti-Stokes components effectively. Figure 2.9(a) illustrates the internal configuration of a Raman spectrometer, while Figure 2.9(b) presents a digital image of the STR 500 Raman spectrometer (Airix Corp) utilized in this study.

2.8 Surface Profiling

Surface profiling is an essential technique for determining the thickness of thin films during device fabrication processes. Among the available methodologies, linear surface profiling is one of the simplest and is commonly performed using a stylus-based profilometer. The stylus, a critical component of the surface profiler, applies a consistent force to the surface being analyzed, controlled by an advanced computerized feedback mechanism.

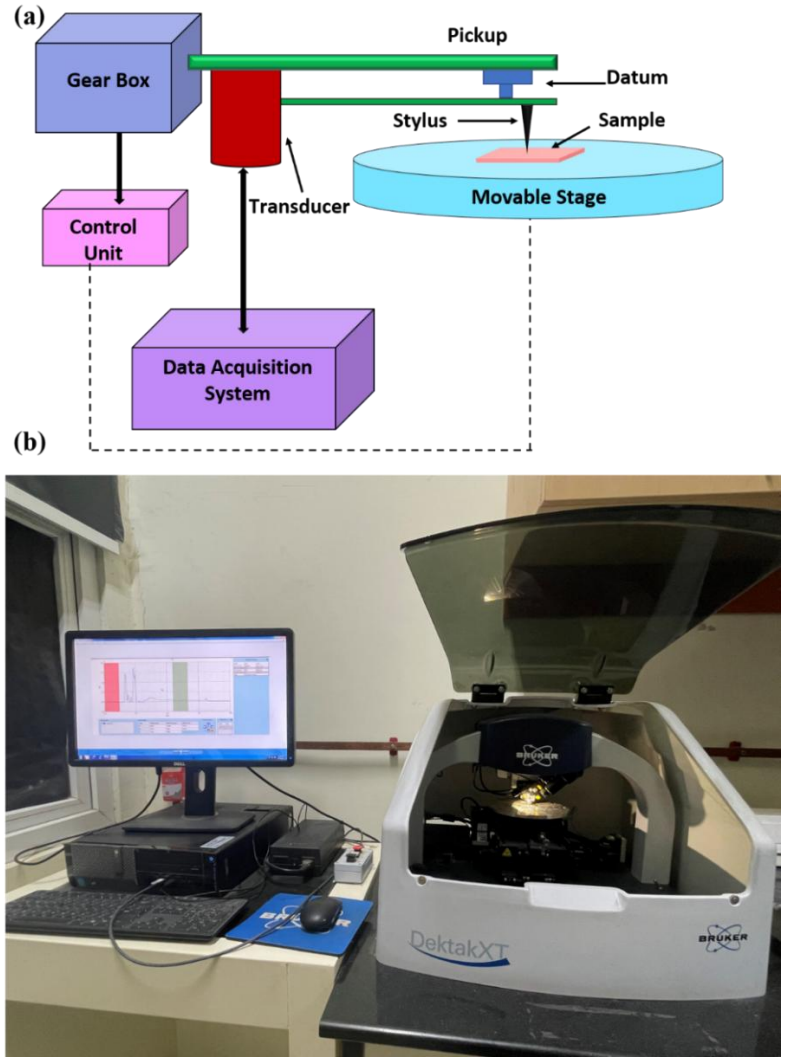


Figure 2.10 (a) Schematic and **(b)** digital image of the Profilometer.

The stylus is mechanically coupled to the profiler system, enabling precise vertical (upward and downward) movement. Film thickness measurements are conducted by scanning the stylus across the sample surface. Variations in surface elevation result in corresponding fluctuations in the applied force, which are detected by the feedback loop and recorded for analysis. This approach, classified as contact-mode profilometry, provides detailed surface profiles by directly interacting with the film. A schematic representation of the profiling technique is shown in Figure 2.10(a). Alternatively, non-contact profilometry uses optical techniques to measure surface profiles without physical interaction, eliminating the risks associated with direct contact. While contact-mode profilometry offers high resolution and accuracy, it has inherent limitations, including potential damage to the stylus tip when scanning abrasive films and reduced scanning speed due to the drag force generated by direct contact. In contrast, non-contact methods are faster and eliminate tip damage but may have lower sensitivity for certain materials. For this research, contact-mode profilometry was employed using the Bruker DekTak-XT surface profiler to measure thin film thicknesses with high precision. The instrument, depicted in Figure 2.10(b), provides reliable results for a range of applications, despite the inherent challenges of the contact-based technique.

2.9 Differential Scanning Calorimetry (DSC)

Differential scanning calorimetry (DSC) is a widely utilized technique in thermal analysis, offering critical insights into the physical and chemical properties of materials. By monitoring heat flow into or out of a sample as a function of temperature or time, DSC enables the study of various thermal phenomena, including phase transitions, glass transitions, chemical reactions, and decomposition processes. The principle of DSC involves measuring the temperature difference (ΔT) between a sample and a reference material as a function of time or temperature. Both the sample and reference are subjected to simultaneous heating or cooling under precisely controlled conditions. During this process, any thermal events occurring in the sample, such as phase transitions or exothermic/endothermic reactions, result in heat absorption or release, causing a measurable change in ΔT. This technique provides a comprehensive understanding of the material's thermal behavior, making it invaluable for material characterization in research and development. The schematic diagram of DSC is shown in Figure 2.11(a). For this research, Perkin Elmor DSC 4200 system is used as depicted in Figure 2.11(b), provides reliable results for a range of applications, despite the inherent challenges of the contact-based technique.

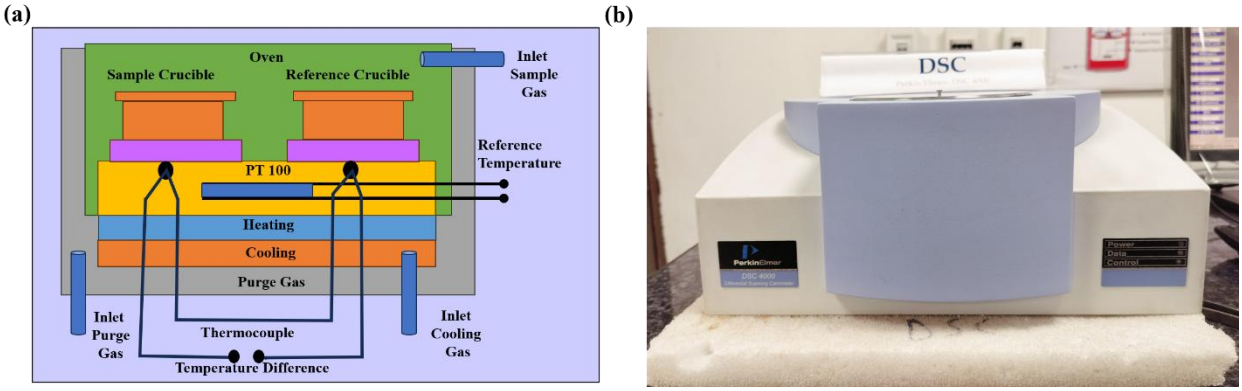


Figure 2.11 (a) Schematic and (b) digital image of the DSC.

2.10 Thermogravimetric analysis (TGA)

TGA is a thermal analysis technique employed to measure changes in the mass of a material as a function of temperature or time under a controlled environment. The analysis is conducted by heating a sample at a programmed rate while continuously monitoring its weight using a high-precision balance. This setup ensures that the balance is protected from extreme temperatures while maintaining accuracy in mass measurements.

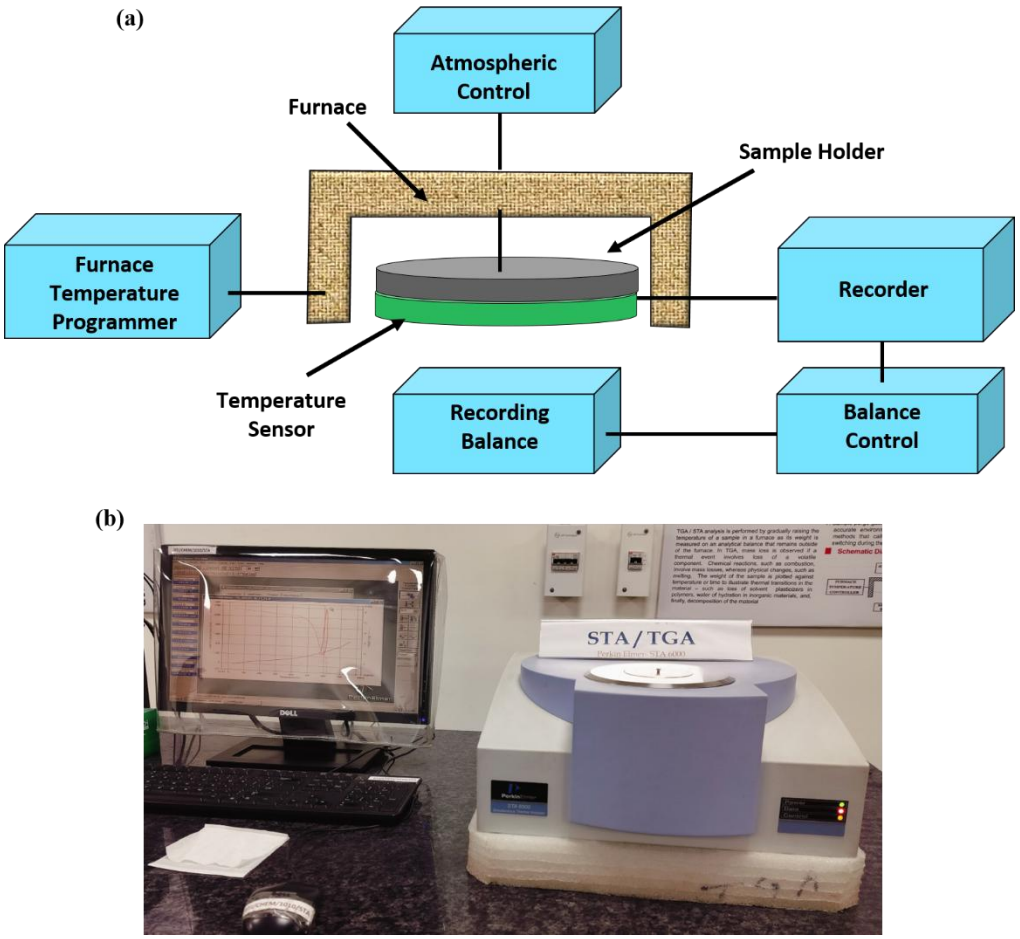


Figure 2.12 (a) Schematic and **(b)** digital image of the TGA.

During a TGA experiment, the sample is exposed to a controlled atmosphere, which may include inert, oxidative, or reducing gases, depending on the study's objectives. As the sample undergoes thermal processes, changes in mass are recorded. Mass loss is typically associated with thermal events involving the evaporation of volatile components, decomposition, or chemical reactions such as oxidation or combustion. Conversely, physical transitions such as melting or crystallization do not usually result in mass changes. The results of a TGA analysis are typically represented as a plot of sample weight versus temperature or time, providing valuable information about the thermal stability, composition, and decomposition behavior of the material. This method is widely used in material science, polymer, 2D materials, and quality control to characterize materials and understand their thermal properties. For this study, the PerkinElmer STA6000 system was utilized to perform TGA analysis, offering precise control over heating rates and atmospheric conditions to ensure accurate characterization of the material's thermal behavior. The schematic diagram of TGA and digital image of PerkinElmer STA6000 system are shown in Figure 2.12(a & b) respectively.

2.11 Electrical Characterization and Parameter Extraction

The electrical properties of the fabricated RRAM devices were investigated using a Keithley 4200 semiconductor characterization system (SCS) with a customized library designed for two-probe measurements, as shown in Figure 2.13(a). This system allowed the devices to be evaluated for their current-voltage (*I-V*) and capacitance-voltage (*C-V*) characteristics. Measurements were conducted using the Keithley Interactive Test Environment (KITE), which enabled control of various parameters, including compliance current, voltage steps, and peak voltages in a dual sweep voltage mode. The devices were tested on a Cascade Microtech PM5 probe station, which features a 150 mm chuck mounted on a new port pneumatic vibration isolation platform, as depicted in Figure 2.13(b). High-precision electrical connections were

achieved using triax coaxial cables that linked the probe station to the source measurement units (SMUs) of the characterization system, ensuring accurate and low-noise measurements. For system-level application, the RRAM device's performance is assessed against multiple parameters, such as fabrication conditions, material properties, and electrical behavior. Additional factors include reliability, repeatability, sample yield, variability, endurance, retention time, and conduction mechanisms. These characteristics directly influence the device's applicability for memory storage or neuromorphic computing. To extract key performance metrics, devices were subjected to various electrical conditions, including sweep voltages, bias voltage, voltage pulses, and thermal conditions. Initial tests involved plotting current versus voltage on a logarithmic scale, showcasing the device's resistive switching characteristics. A representative graph is shown in Figure 2.14(a), illustrating the bipolar resistive switching behavior of the device.

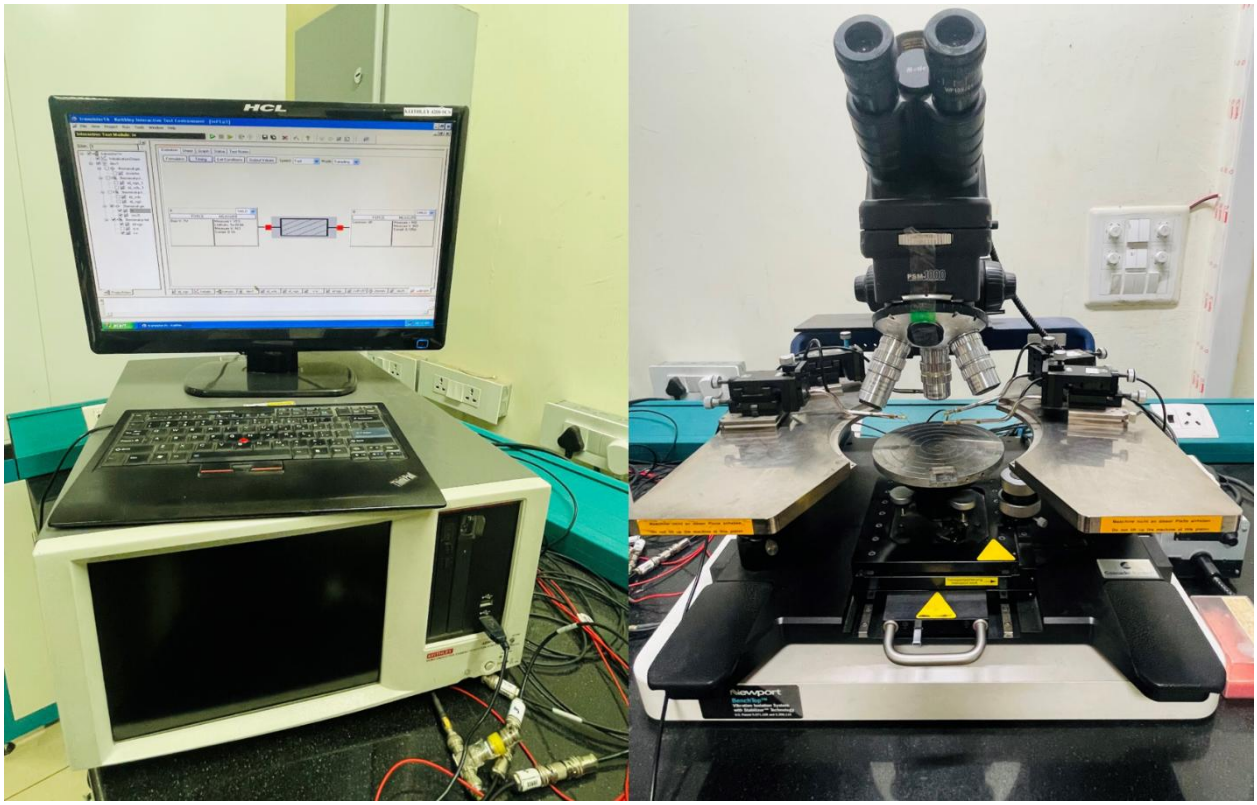


Figure 2.13 (a) Schematic and **(b)** digital image of the SCS 4200.

During testing, the TE (TE) was connected to the applied voltage, while the BE was grounded. The voltage sequence of 0 → V_{max} → 0 was applied across the TE and BE with an appropriate compliance current. As the voltage increased in the positive range, a significant rise in current was observed at the set voltage (V_{SET}), transitioning the device to LRS as shown in Figure 2.14(a). This transition was caused by the migration of metal ions from the TE to the BE under a strong electric field, confirming the formation of a metallic filament within the switching layer. Once the RRAM devices reach to LRS, a negative voltage sequence (0 → -V_{max} → 0 was applied to switch the device back to the HRS. A sharp drop in current was observed at the reset voltage (V_{RESET}), indicating a return to HRS. This behavior is attributed to the rupture of the conductive filament formed during the set process. The memory window, defined as the ratio I_{ON}/I_{OFF} was determined at a specific read voltage to ensure stability and minimize the impact of external noise or repeated switching cycles. This characterization approach provides detailed insights into the resistive switching behavior, operational stability, and performance of RRAM devices, confirming their potential for advanced memory applications. To further assess the reliability of these switching behaviors, the endurance of the device is evaluated using two primary characterization techniques. The first method, DC endurance measurement, involves repeating multiple switching cycles under controlled voltage sweeps to observe the consistency

of the device's switching characteristics. This approach, as depicted in Figure 2.14(b), helps determine basic endurance parameters but does not accurately capture the actual endurance limits or the switching speed of the device. Alternatively, the second method employs a high-speed pulse train, typically following a set-read-reset-read sequence, using square or triangular waveforms. This technique enables real-time monitoring of current after each transition between HRS and LRS, providing insights into the device's ability to sustain rapid switching cycles. An endurance failure in this context is identified when the device fails to either set or reset, indicating degradation in its operational performance over time.

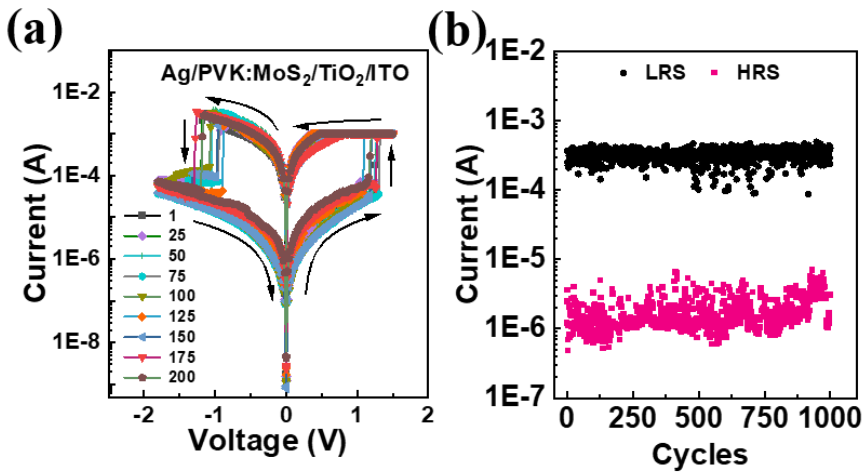


Figure 2.14 (a) *I-V* characteristics of flexible RRAM device with V_{SET}/V_{RESET} of ~1 V/-1.5 V. **(b)** The DC endurance of 1000 switching operation at read voltage of 0.2 V.

Retention time is another critical parameter for evaluating the reliability of non-volatile memory devices. In this study, the retention time was determined by first switching the device to a specific resistance state which is either HRS or LRS. Once the device was set to the desired state, a constant read voltage of 0.2 V was applied, and the corresponding current was measured over a long duration of time. In retention characteristics, the current values for both states were then combined and plotted on a single curve for comparison. To assess long-term retention, the data were taken at 85 °C and extrapolated to simulate a period of at least 10 years. Linear fitting was applied to determine the slope of the current decay for both states, providing insights into the stability of the resistance difference over time. The extrapolated results offer a predictive analysis of the duration for which a clear distinction between HRS and LRS can be reliably maintained. Further, the activation energy (EA) for both the HRS and LRS was determined by performing a linear fit of the logarithm of the current (log I) versus the reciprocal temperature ($1/kT$) plot. In this context, k represents the Boltzmann constant, and T denotes the absolute temperature in kelvin. A lower value of EA indicates that less energy is required for transitions between the states. The cycle-to-cycle variability is other parameter to study the reliability of RRAM. The Weibull distribution is a widely utilized statistical method for analyzing cycle-to-cycle variations in both resistance states (LRS and HRS) and operating voltages (SET and RESET). This approach provides a robust framework for assessing the reliability and consistency of device performance. The variation coefficient (CV) is a statistical measure used to quantify the relative variability or dispersion of a dataset relative to its mean. It is calculated using the following formula:

$$CV = \frac{Standard\ Deviation}{Mean} \times 100 \qquad (2.1)$$

A lower value of CV signifies greater consistency in the data, whereas a higher CV indicates increased variability.